NON INVASIVE OPTICAL SYNCHROTRON RADIATION MONITOR USING A MINI-CHICANE

R. Fiorito, R. Kishek, A. Shkvarunets, University of Maryland, College Park, MD, USA
D. Castronovo, M. Cornacchia, S. Di Mitri, M. Veronese, ELETTRA-Sincrotrone Trieste, Italy
C. Tschalaer, MIT, Cambridge, MA, USA

Abstract

We are developing a design for a minimally perturbing mini-chicane, which utilizes the optical synchrotron radiation (OSR) generated from magnetic bends, to measure the rms transverse emittance and other optical parameters of the beam. The beam is first externally focused at the first bend and the OSR generated there is used to image the beam. Subsequently, pairs of bends produce interferences (OSRI) whose visibility can be used to determine the beam divergence or the energy spread. The properties of different configuration of bends in the chicane have been analyzed to provide an optimum diagnostic design for a given set of beam parameters which: 1) provides a sufficient number of OSRI fringes to allow a measurement of the beam divergence; 2) minimizes or maximizes the competing effect of energy spread on the fringe visibility; 3) minimizes the effect of coherent synchrotron radiation and space charge on the beam emittance; and 4) minimizes the effect of compression on the bunch length, as the beam passes through the chicane. Diagnostic designs have been produced for 100-300 MeV beams with a normalized rms emittance of about 1 micron for application to Fermi@Elettra and similar high brightness free electron lasers.

INTRODUCTION

OSR and optical edge radiation interferences from magnetic bends and field transitions have been studied and used to measure electron beam size and divergence at storage rings and linacs [1-4].

To develop these ideas further we have developed a computer code [4] that can specifically calculate the angular distribution of SR in the far field radiated by electron moving along a specified curved trajectory. We have applied this code to calculate OSR interferences and study the effect of beams with divergence and energy spread on the resulting OSR interferences from two magnetic dipoles separated by a distance L as is shown in Figure 1. The two magnetic dipole fields can be oriented such that the trajectory follows either a 'U' or an 'S' shape as indicated.

Figure 2 shows that for the 'U' configuration the SR from the two magnets overlap and thus interfere only in a limited angular region ($\Delta\theta \sim 3 / \gamma$). To the contrary, in the 'S' configuration the SR from the two sources completely overlap and the angular region of observable interference is much larger than in the 'U' case. The visibility of the interferences in both systems is affected by beam divergence and energy spread and, for different pairs of
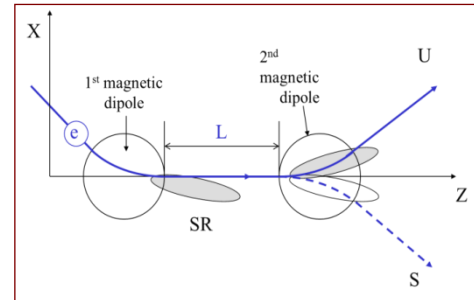

Figure 1: Geometries for generation of synchrotron radiation from two magnetic dipoles in a 'U' or 'S' configuration.
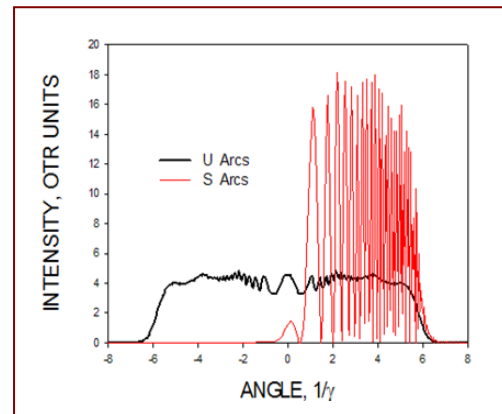

Figure 2: Far field interference patterns for 'U' (black) and 'S' geometries (red) shown in Figure 1.

magnets, the corresponding interferences can be used to measure either of these quantities, as we shall see below.

The chief goal of this work is to develop a non-invasive OSR emittance monitor (NIEM) diagnostic system that can measure normalized emittances in the range of ~1 micron, i.e. that are typically produced by state of the art photo-injector driven free electron lasers (FELs). To accomplish this we have developed a design for a compact mini-chicane which uses small electromagnets to perturb the beam trajectories just enough to produce OSR and OSR interferences. These radiations can be used to diagnose the beam size and divergence in the bending plane. The chicane then returns the beam to its original trajectory axis.

In this paper we describe the features and expected performance of a NIEM diagnostic. In particular we have examined in detail the application of such a diagnostic at two energies (100 and 285 MeV) for the FERMI@Elettra accelerator [5]. This design study can provide a benchmark for other similar accelerators.

NIEM DESIGN STUDY

Chicane Design

A sketch of the chicane that we plan to use for the NIEM is shown in Figure 3.
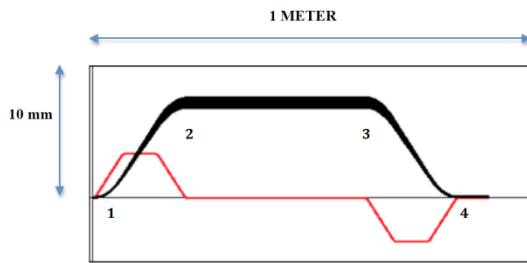
Figure 3: Schematic of diagnostic chicane showing electron trajectories (black) and deflection angles (red).

The first two magnetic bends (1,2) of the chicane form an 'S' type interferometer that is used to monitor the energy spread; and the second and third bends (2,3) form a 'U' interferometer that is used to measure the beam divergence. Figure 3 shows the trajectories (black lines) and deflection angles (red) of the beam electrons as they pass through the chicane. Note the very small (7 mm) vertical shift of the trajectories (shown in black) from the axis in comparison to the horizontal separation of bends (2,3) (i.e. 0.6 m). Each dipole in the chicane is 0.1 m long with a bending angle of 35 mrad (shown in red).

Emittance Measurement Technique

The rms beam emittance will be determined by magnetically focusing the beam at the first bend of the chicane with external quadrupoles upstream of the diagnostics chicane. An optical imaging system focused on the OSR from this bend will observe the beam here. Two other imaging systems will independently observe the far field radiation OSR interference patterns from bends (1,2) and (2,3) respectively, to obtain the beam energy spread and divergence similar to what is done with optical transition radiation [6-9].

The beam size and divergence data will be processed to obtain the emittance using a new methodology that we have recently developed [10]. When this approach is applied to a beam with negligible space charge, the emittance for either the horizontal or vertical plane can be given in a closed form in terms of the beam size and divergence measured, respectively, at a beam size or divergence minimum.

Alternatively, any two values of divergence and radius taken at different focusing strengths can be used to determine the emittance. These measurements do not necessarily need to be at or even close to a minimum in either parameter. This method is particularly advantageous when the range of magnetic focusing is limited. Furthermore, the statistical accuracy of the measurement of the emittance can be improved by using several pairs of values and the method can be applied to beams with significant space charge as well as emittance

dominated beams. The method has been tested using simulated data and there is excellent agreement between WARP simulations and calculations [10].

Beam Line Locations and NIEM Parameters

We have designed chicanes that can be used to monitor the emittance at two locations of interest. The first location is just upstream of a laser heater system at FERMI [11] that is designed to suppress any micro-bunching. This process is produced by energy modulations arising from longitudinal space charge (LSC) fluctuations. The beam energy here is 100 MeV. This point is interesting because from this energy onward transverse space charge effects are negligible and, in absence of other perturbations (e.g. CSR, wakes, chromatic effects, etc., all of which are minimized as much as possible in the FERMI design), the normalized emittances should remain constant. This is also the point before bunch compression, where the bunch is long and the correlated and uncorrelated energy spreads are small. Because of these two situations one expects little disruption to the bunch from the NIEM.

A second location of interest for a NIEM device is after the 1st bunch compressor where the beam energy is 285 MeV. This is an interesting region because a NIEM here can observe any possible emittance blow up that might have occurred in the compressor chicane. This location presents a more delicate beam dynamics situation, since the bunch will traverse the NIEM with the large correlated energy spread (<=2%) that is required by the preceding bunch compressor.

The parameters of the chicanes for these two locations are: 1) a magnetic field strength, $B = 0.12$ Tesla for 100 MeV and 0.35 Tesla for 285 MeV; 2) magnet length, l =100mm; and spacing, L= 0.6m, between magnets (2,3). These parameters are required to easily measure both the divergence and the beam size for normalized emittances in the range of 1 to several microns.

We have also determined that the energy spreads expected at each of these energies (0.005 and 0.02 respectively) can also be measured by independently observing the OSR interferences from magnets (1,2).

As an example, we show the results of our OSRI calculations using the above parameters for 100 MeV. However, the code results demonstrate similar sensitivities to divergence and energy spread for 285 MeV as well.

Divergence and Energy Spread Calculations

Figure 4 shows that a beam divergence of 70 microrad can easily be measured with OSRI from magnets (2,3) in the presence of the expected rms energy spread at FERMI@Elettra, at 100 MeV, which is 0.5 MeV. Note that (2,3) form a 'U' type interferometer, as shown in Figure 3, where the interference from the two sources are clearly visible only in a limited angular region; this is shown by the fall off of the fringe amplitudes at angles greater than a few times $1/\gamma$. In addition, because of the small angular dispersion in the region between (2,3) there
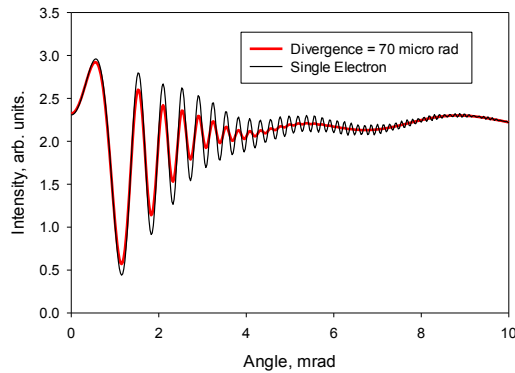
Figure 4: OSR interferences from magnets (2,3) showing the fringe visibility for single electron (black) and a beam with divergence = 70 micro radians (red).

is practically no effect of energy spread on the OSRI patterns; we have verified this by calculation and it is seen by the nearly parallel electron trajectories between bends (2,3) shown in Figure 3. Our simulations show that it should be possible to measure divergence with the (2,3) interferometer to about 50 microrad.

Figure 5 shows that the fractional energy spread (0.005) severely alters the fringe visibility of OSRI from magnets (1,2). In fact, the energy spread dominates over the effect of the same value of divergence (70 microrad), which dominates the visibility of the fringes from (2,3) as shown in Figure 4. This is due to the large angular dispersion in the region between (1,2) and is visible in the divergence of the trajectories shown in Figure 3. Thus, we conclude that interferometer (2,3) and (1,2) can be used to measure the divergence and energy spread, respectively.
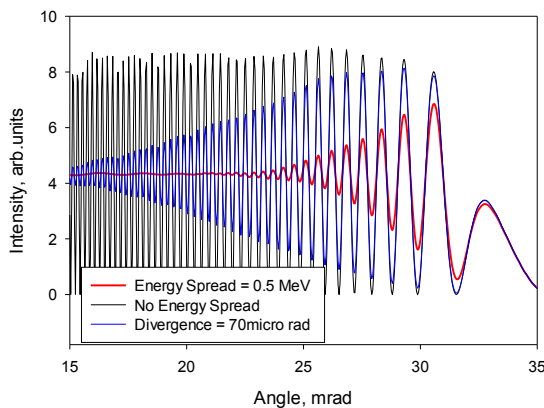

Figure 5: OSRI from magnets (1,2) showing how the fringes (black curve) are affected by energy spread (red curve) and divergence (blue curve).

Beam Size Estimate

The transverse size of the beam must also be measured to determine the beam emittance. The beam size usually is characterized by its RMS value (σ_b), meaning that the beam profile is approximated by a normal distribution function, i.e. a Gaussian function: $\exp\left(-x^2/2\sigma_b^2\right)$ where

σ_b is the one dimensional RMS value of this function. In order to calculate the beam emittance we are interested in the measurement of the RMS beam size from the OSR radiation produced by the beam rather than its detailed profile.

The resolution limit which limits the beam size measurement is the point spread function (PSF), which for OSR can be defined as the distribution of the OSR produced by a *single electron* seen by the imaging optics in the image plane. We can again characterize the PSF in the same terms as we characterized the beam profile above, i.e. by its RMS value σ_{PSF}, assuming the PSF is approximately Gaussian. If the measured SR distribution produced by the entire beam is likewise characterized and has a RMS value, σ_m then $\sigma_b^2 = \sigma_m^2 - \sigma_{PSF}^2$.

A simple estimate of the RMS value of the PSF can be made by assuming that the vertical and horizontal distributions of the OSR light are nearly equal (horizontal aperture used) and can be described by a Gaussian with an RMS value of $0.2/\gamma$. The above estimate is maximal and it is based on the facts that a) the RMS of the PSF becomes larger the smaller the angular size of the radiation pattern; and b) that the smallest angular size of OSR is in the vertical direction.

Then for an optics system with magnification $m = 1$, the RMS of the PSF $\sigma_{PSF} \approx 1.6\gamma\lambda$. For example, for an electron with energy 100MeV and an observation of λ=400 nm, the RMS of the PSF $\sigma_{PSF} \approx 100\mu$m. If the measured size of the OSR spot is significantly greater than this value, it is straightforward to estimate the rms beam size. However, if it is comparable, the PSF will limit the measurement and another technique, e.g. which measures the beam size via a measurement of the transverse optical coherence function, must be employed [12]. This is likely the case for the higher beam energy of 285 MeV.

Beam Dynamics in the Chicane

The NIEM chicane has the physical configuration of a typical magnetic bunch compressor and poses the same potential threats to the electron beam emittance: 1) emission of coherent synchrotron radiation (CSR) and its associated increased projected horizontal emittance and energy spread; 2) an enhancement of the micro-bunching instability driven by longitudinal space charge (LSC); 3) direct space charge effects at energies ≤ 100 MeV. Also, contrary to a bunch compressor chicane, a diagnostics chicane must not alter the bunch length. In order to study these effects, we have run both ELEGANT [13] and WARP [14] simulations for the two positions and energies of interest to FERMI.

Table 1 shows the ELEGANT predictions for the normalized emittances, bunch length and fractional energy spread (all RMS) at the entrance and exit of NIEM for the 100 MeV and 285 MeV cases for the FERMI bunch charge, which is 0.5 nC. The simulations predict that the NIEM will leave the beam characteristics essentially unchanged at either position.

Table 1: Beam Parameters Before and After the NIEM Chicane Computed from ELEGANT Simulations

Energy (MeV)	Position in the chicane	Horiz. emit. (mm-mrad)	Vert. emit. (mm-mrad)	Bunch length (mm)	Energy Spread
100	entrance	1.00	1.00	1.00	0.005
	exit	1.00	1.00	1.00	0.005
285	entrance	1.05	1.06	0.18	0.020
	exit	1.05	1.08	0.17	0.020

The effect of space charge on the transverse beam emittance has also been estimated using the WARP simulation code. The results show that space charge at a peak beam current of 130A will have a negligible effect on the emittance; and, furthermore, that one has to go up to 1 kA peak current (1 nC in 1 ps) to see appreciable space charge effects, i.e. a 1.25% change in the emittance and a 26.4% change in the beam radius. The peak current for FERMI (0.5 nC in a 13.4 ps bunch) is ~ 50A.

Moreover, theory predicts that the LSC-driven micro-bunching gain due to the NIEM only, at both energies, is of the order of unity (1-D linear model, analytical). The bunch length is unchanged by NIEM because the geometry and bending angles of NIEM give very little change in path length with energy deviation (R56 in transport matrix terms). Also for this reason, LSC-driven micro-bunching is estimated to have gain close to unity (i.e. there will be no amplification in the NIEM).

CONCLUSIONS

We have evaluated a design for a non interceptive emittance and energy spread diagnostic chicane (NIEM) to measure the beam properties of high quality electron beam accelerators with rms emittances ~ 1 micron. In particular we have evaluated a NIEM diagnostic for use at the FERMI FEL. Our OSR codes show that our design can measure the expected the beam divergence and energy spreads typically produced at two points in the FERMI beamline, i.e. at 100 and 285 MeV.

ELEGANT and WARP simulations additionally show that introduction of the NIEM chicane into the beam line leads to minimal emittance blow up due to CSR, energy spread and space charge as well as minimal bunch compression. Thus, we conclude that NIEM meets the requirements for a non-invasive emittance monitor for a typical, high quality electron beam accelerator.

In future studies we will provide a more precise calculation of the PSF of the OSR beam imaging system as well as develop the measurement optics necessary to isolate the OSR interferences from each pair of magnetic bends.

ACKNOWLEDGEMENT

REFERENCES

[1] O. Chubar, *Rev. Sci. Instruments*, 66, 1872, (1995)

[2] N. Smolykov, *Nuc. Instrum. and Methods B*, 448, 73 (2000).

[3] N. Smolykov, *Nuc. Instrum. and Methods A*, 543, 51 (2005).

[4] A. Shkvarunets and R. Fiorito, "Optical Synchrotron and Edge Radiation Diagnostics for Relativistic Electron Beams", *AIP Conf. Proc. No. 732*, edited by T. Shea and R. Shipley (AIP, New York, 2004), pp. 429–436

[5] C.J. Bocchetta, et al., FERMI@Elettra FEL Conceptual Design Report, http://www.elettra.trieste.it/FERMI (2007)

[6] R. B. Fiorito, D.W. Rule, "Optical Transition Radiation Beam Emittance Diagnostics", *AIP Conf. Proc. No. 319* (AIP, New York, 1994), p. 21

[7] R. B. Fiorito, A. G. Shkvarunets, T. Watanabe, V. Yakimenko, D. Snyder, *Phys. Rev. ST Accel. Beams* 9, 052802 (2006)

[8] M. Holloway, R. B. Fiorito, A. G. Shkvarunets, S.V. Benson, D. Douglas, P. Evtushenko, K. Jordan, *Phys. Rev. ST Accel. Beams* 11, 082801 (2008)

[9] R. Fiorit, A. Shkvarunets, "Use of Optical Transition Radiation Interferometry for Energy Spread and Divergence Measurements", p. 89, Proc. of DIPAC03, Mainz, Germany (2003)

[10] K. Poorrezaei, R. Fiorito, R. Kishek, B. Beaudoin, *Phys. Rev. ST Accel. Beams*, 16, 082801 (2013)

[11] S. Spampinati, et al., "Progress with the FERMI Laser Heater Commissioning", WEPSO67, Proc. of FEL13, New York, NY (2013)

[12] T. Naito, T. Mitsuhashi, *Phys. Rev. ST Accel. and Beams*, 9, 122802 (2006)

[13] M. Borland, "ELEGANT: A Flexible SDDS-Compliant Code for Accelerator Simulations", Advanced Photon Source LS-287, September (2000)

[14] D. P. Grote, A. Friedman, I. Haber, Fusion Eng. Des. 32–33, 193 (1996); J.-L. Vay, *Phys. Rev. Lett.* 98, 130405 (2007)